


## Copula-based modeling of hydraulic structures using a nonlinear reservoir model

Qiaofeng Tan, Yunze Mao , Xin Wen\*, Tian Jin, Ziyu Ding and Zhenni Wang

College of Water Conservancy and Hydropower Engineering, Hohai University, Nanjing 210098, China

\*Corresponding author. E-mail: njwenxin@163.com

 YM, 0000-0001-6611-7074

### ABSTRACT

Multivariate flood frequency analysis has been widely used in the design and risk assessment of hydraulic structures. However, analytical solutions are often obtained based on an idealized linear reservoir model in which a linear routing process is assumed, and consequently, the flood risk is likely to be over- or underestimated. The present study proposes a nonlinear reservoir model in which the relationships of reservoir water level with reservoir volume and discharge are assumed to be nonlinear in order to more accurately describe the routing process as it takes into consideration the interactions between hydrological loading and different discharge structures. The structure return period is calculated based on the copula function and compared with that based on the linear reservoir model and the bivariate return period based on the Kendall distribution function. The results show that the structure return period based on the linear model leads to an underestimation of the flood risk under the conditions of high reservoir water level. For the same reservoir, linear and nonlinear reservoir models give quite different reservoir volume-water level and discharge-water level curves; therefore, they differ substantially in the sensitivity to flood events with different combinations of flood peak and volume. We also analyze the effects of the parameters involved in the reservoir volume-water level and discharge-water level relationships on the maximum water level at different return periods in order to better understand the applicability and effectiveness of the proposed method for different hydraulic projects.

**Key words:** bivariate flood frequency analysis, copula, nonlinear reservoir model, structure return period

### HIGHLIGHTS

- The structure return period is calculated based on the nonlinear reservoir model.
- Nonlinear relationships of water level with volume and discharge are assumed.
- Interactions between hydrological loading and different structures are analyzed.
- Effects of different storage and discharge capacity parameters are discussed.

## 1. INTRODUCTION

An extreme hydrological event is considered a major cause of hydraulic structure failure, and thus, its occurrence probability provides an important basis for the evaluation of the structure return period in the design of hydraulic structures. Thus, it is important to choose appropriate variables and methods for the risk assessment of an extreme hydrological event acting on the hydraulic structures. However, the widely used univariate flood frequency analysis does not account for the interactions between hydrological events and hydraulic structures. The extreme load that can be supported by a hydraulic structure in a flood event is determined by the storage and routing processes, and changes in any characteristic variable of the flood event, such as flood peak, volume and duration, and the hydraulic structure, can have a substantial effect on the extreme load.

In univariate flood frequency analysis, the return period of a given hydrological variable is taken as the return period of structural failure. It is evident that the univariate return period of the flood peak or volume cannot provide a complete evaluation of the occurrence probability of hydrological events (Chebana & Ouarda 2011), which therefore may result in over- or underestimation of the flood risk and hydraulic design standard (Salvadori & De Michele 2004). Apparently, multivariate flood frequency analysis is preferred over univariate flood frequency analysis in hydraulic design. However, a number of drawbacks have also been identified in previous literature. For instance, a normal distribution is often assumed for non-normally distributed flood peak and volume in multivariate normal distribution and normal transformation methods.

This is an Open Access article distributed under the terms of the Creative Commons Attribution Licence (CC BY 4.0), which permits copying, adaptation and redistribution, provided the original work is properly cited (<http://creativecommons.org/licenses/by/4.0/>).

Some marginal distributions may be combined to form a joint distribution, such as bivariate lognormal distribution, bivariate exponential distribution, bivariate Gumbel distribution, and two-dimensional P-III distribution. However, it is generally assumed that the marginal distributions should come from the same family of distributions.

Recently, the Copula function has been widely used in hydrology, especially in multivariate flood frequency analysis. The copula is a function that links univariate distribution functions to a multivariate distribution function describing the dependence among correlated variables (Nelsen 2006). However, there is no universally agreed method for calculating the multivariate return period based on the copula function. Salvadori & De Michele (2004) investigated both unconditional and conditional return periods of hydrological events using copulas, and they found that it was possible to combine the marginal events in several ways using the (inclusive) OR operator and the AND operator. Salvadori *et al.* (2011) introduced another return period, the secondary return period (also called the Kendall return period), which was associated with the realization of dangerous events for the dam. It should be noted that the return periods mentioned above are defined based on the natural occurrence probability of floods. However, the climate changes and human activities in recent years may make the hydrological extreme value series highly non-stationary. For the frequency analysis of non-stationary hydrological extreme value series in a changing environment, the return period should be redefined and several non-stationary methods have been developed, such as expected waiting time, expected number of exceedances, equivalent reliability, and average design life level (Yan *et al.* 2017, 2020).

However, the return period of hydraulic structures should be defined in terms of the risk of dam overtopping or the downstream loss. In multivariate cases, structural failure is considered to be the result of the complex interactions between the structure and the hydrological loads acting on the structure, which indicates that the effects of the reservoir and dam on the inflow hydrographs should also be taken into consideration (Mediero *et al.* 2010). The relationships between hydrological and structure variables can be simulated using observed data. De Michele *et al.* (2005) generated peak-volume pairs using Gumbel copula in order to verify that the maximum water level reached at the dam by the generated hydrographs was below the crest level. Klein *et al.* (2010) proposed a methodology to categorize flood events for risk-based analysis and the design of flood control systems using copulas, and the maximum water level reached at the dam was estimated to graphically analyze its relation with the primary return period for each event. Requena *et al.* (2013) compared the multivariate return period of the hydrological loads with the structure return period by simulation.

An idealized reservoir model can also be established to simulate the relationships between hydrological and structure variables. Notably, the reservoir volume-water level and discharge-water level relationships are assumed to be linear due to the inherent difficulties in mathematical derivation. For instance, Volpi & Flori (2014) proposed an idealized reservoir model in which the reservoir volume-water level and discharge-water level relationships were assumed to be linear and the inflow process was assumed to be constant, based on which the relationships of the maximum discharge with flood peak and volume were derived. Balistocchi *et al.* (2017) proposed triangular hydrographs by assuming linear reservoir volume-water level and discharge-water level relationships. However, the reservoir volume-water level and discharge-water level relationships are more likely to be nonlinear rather than linear in actual reservoir operation depending on the hydraulic structures such as sluice gates, overflow weirs, and orifices. Thus, linearization can lead to over- or under-estimation of the structure return period and flood risk.

The main purpose of the present study is to determine the relationships of the maximum water level at the dam with flood peak and volume by assuming nonlinear reservoir volume-water level and discharge-water level relationships and to develop a methodology for calculating the structure return period based on the copula function. The rest of this paper is organized as follows. In Section 2, we illustrate the structure-based nonlinear multivariate approach for hydraulic structure design and risk assessment. For simplicity, only the bivariate case is considered here. In Section 3, we develop an idealized nonlinear reservoir model, based on which the calculation method of the structure return period is derived. In Section 4, the structure return period based on the nonlinear reservoir model is calculated and then compared with that based on the linear reservoir model and the bivariate return period based on the Kendall distribution function. In Section 5, we discuss the effects of the discharge and storage capacity of the reservoir on the return period. Finally, the main conclusions are drawn in Section 6.

## 2. DEFINITION OF RETURN PERIOD

### 2.1. Return period

The return period is used in hydrology to estimate the recurrence interval of a hydrological event such as flood, rainstorm, and extremely high or low water level with the severity or duration greater than or equal to a given value.

In univariate analysis,  $X$  is a random variable that measures the hydrological loads such as flood peak or volume, and  $F_X$  is the probability distribution function of  $X$ . The occurrence of  $X$  is assumed to be time-independent. The return period of  $\{X > x\}$  is expressed as  $T(x) = \mu/[1 - F_X(x)]$ , where  $\mu$  is the average time interval between two successive occurrences of the hydrological event  $X$  ( $\mu = 1$  year in the case of annual maxima).

In multivariate analysis, some or several hydrological parameters are taken into consideration. For simplicity, only the bivariate case is considered in this study. Let  $X$  and  $Y$  be two random hydrological variables that measure the hydrological processes acting on the structure (e.g., flood peak and volume), and  $F_{X,Y}$  be the joint cumulative probability distribution function of  $X$  and  $Y$ :

$$F_{X,Y}(x, y) = P_r[(X < x) \cap (Y < y)] \quad (1)$$

The joint probability density function  $f_{X,Y}$  can be described as follows:

$$f_{X,Y}(x, y) = \frac{\partial^2 F_{X,Y}(x, y)}{\partial x \partial y} \quad (2)$$

provided that  $f_{X,Y}$  does exist.

## 2.2. Estimation of the bivariate return period by copulas

Copula has emerged as a useful tool for multivariate hydrological frequency analysis, and the Archimedean and extreme value copula families are most often used for modeling flood variables. A distinct property of Archimedean copulas is that they can be constructed easily and allow for a great variety of dependence structures. Archimedean copulas such as Frank copula (Favre *et al.* 2004) and Clayton copula (Shiau *et al.* 2006) have been widely used to characterize the dependence structure between peak and volume variables. Extreme value copulas are able to connect the extreme values of the studied variables, which are very important in flood frequency analysis. The Gumbel copula is considered to best represent the relationship between peak and volume (Zhang & Singh 2006). Many bivariate return periods have been estimated by copulas in recent years, and the most representative ones are the 'AND' return period and the Kendall return period.

For a given critical probability level  $p$ , the 'AND' return period is described as:

$$\theta = \frac{\mu}{1-p} = \frac{\mu}{1 - F_{X,Y}(x_p, y_p)} \quad (3)$$

where  $x_p$  and  $y_p$  are the coordinate pairs of any point on the critical level curve  $L_p$ .

The critical level curve  $L_p$  is the set of points corresponding to the probability level  $p$ ,  $L_p = \{(x, y) \in R^2 | F_{X,Y}(x, y) = p\}$ , and the corresponding supercritical region is given by  $\hat{D}_p = \{(x, y) \in R^2 | (x > x_p) \cup (y > y_p)\}$ , in which  $X$  and  $Y$  can be infinite, and the coordinate pairs of  $x_p$  and  $y_p$  on the critical level curve  $L_p$  represent the probability  $p$ .

The Kendall return period is defined in order to identify the univariate critical threshold in a multivariate context (Salvadori *et al.* 2013), and it is described as:

$$\theta_K = \frac{\mu}{1 - K(p)} \quad (4)$$

where  $K(p)$  is the Kendall distribution function obtained from the joint distribution function  $F_{X,Y}$ , which is expressed as  $K(p) = \Pr[F_{X,Y}(x, y) \leq p]$ .  $K(p)$  is greater than or equal to  $K$ , and then  $\theta_K \geq \theta$ . This return period represents the average inter-arrival time of random variables  $X$  and  $Y$  in the supercritical region  $\hat{D}_K$ ,  $\hat{D}_K = \{(x, y) \in R^2 | F_{X,Y}(x, y) > p\}$ . The critical level curve can be further improved based on the 'AND' return period, which is thus referred to as the secondary return period.

## 2.3. Structure return period

The concept of structure return period is inspired by the supercritical region of the Kendall return period. It is noted that both 'AND' and Kendall return periods account only for the natural occurrence of floods, while the structure return period takes into consideration the response of hydraulic structures of the reservoir to floods. In this case, the critical level depends critically on the consistent responses of the hydraulic structures, and the supercritical region is the region over the structure response isoline.

$Z$  is defined as the design parameter characterizing a hydraulic structure (e.g., the dimension of the spillway and the elevation of the levee) or variables associated with the structure. In actual applications,  $Z$  indicates the effect of hydrological loads acting on the structure. There is a strictly monotonically increasing function between  $Z$  and hydrological load  $X$  in a univariate case. The structure function is  $Z = g(x)$ , where there exists a unique inverse function  $g^{-1}$ . Note that this assumption holds for all hydraulic structures. In a univariate case, the probability distribution function of  $Z$  is the same as that of  $X$ , and thus  $F_Z(z) = F_X(x)$ , where  $x = g^{-1}(z)$ . Then, the return period of  $Z$  is the same as that of  $X$ , both of which can be used in the evaluation of hydrological events.

In a bivariate case, the structure design parameter  $Z$  depends on two hydrologic variables,  $X$  and  $Y$ , where  $Z = g(X, Y)$ , and the structure function  $g(X, Y)$  takes into consideration the interactions of the structure and the hydrological load acting on the structure. The joint probability distribution function of  $Z$  can be derived from the following equation:

$$F_Z(z) = \int_{D_Z} f_{X,Y}(x, y) dx dy \quad (5)$$

where  $D_Z$  is the region of the  $XY$  plane that satisfies  $g(x, y) \leq z$ . In order to obtain  $F_Z(z)$ , there is a need to find the upper integral of  $D_Z$  for each  $z$ .

The return period of structural failure can be easily obtained by using the standard univariate frequency analysis of the random variable  $Z$ ,  $T(z) = \mu/[1 - F_Z(z)]$ , which is the average time interval between two successive events in the same supercritical region  $\hat{D}_Z = \{(x, y) \in R^2 | g(x, y) > z\}$ . A vector of the design parameter  $Z$  can also be obtained from the return period, and the expression of  $D_Z$  may be very complex in this case. Thus, only a single design variable  $Z$  is considered in this study for the sake of simplicity.

Then, the design parameter quantile in multivariate design can be determined:

$$z_T = F_Z^{-1}\left(\frac{1 - \mu}{T}\right) \quad (6)$$

where  $F_Z$  can be determined by Equation (5).

Here, the objective of hydrological design is to determine the combination of  $x_p$  and  $y_p$  pairs in a given supercritical region at a given failure probability  $p$ . The supercritical regions may differ substantially in terms of their boundaries, which is closely associated with the structure under consideration and associated variables. The boundary of the supercritical region  $\hat{D}_Z$  can be determined by the structure function  $g(x, y)$  described in Equation (5), which represents the hydrological load–structure interactions. Thus, it is imperative to consider the structure and the way it interacts with the hydrological load in determining the suitable structure function  $g(x, y)$ . However, it is noted that the expression of  $g(x, y)$  is too complex to be described mathematically in many actual cases, and thus, there is a need to obtain the analytical solutions in a simpler and more efficient fashion.

### 3. NONLINEAR STRUCTURE MODELING

It is clear that the structure function  $g(x, y)$  that can more accurately capture the interactions between the structure and the hydrological load acting on the structure plays a key role in calculating the structure return period. Given the complexity in mathematical derivation, an idealized reservoir model was proposed in previous studies of Volpi & Flori (2014) and Balistocchi *et al.* (2017), where the reservoir volume–water level and discharge–water level relationships were assumed to be linear. However, both of them are likely to be nonlinear rather than linear in actual reservoir operation depending on the combinations of different drainage facilities such as sluice gates, overflow weirs, orifices and hydraulic turbines, as shown in Figure 1. Thus, this study focuses on the structure return period based on a nonlinear reservoir model. First, a nonlinear reservoir model is developed. Then, reservoir operation is simulated for different inflow hydrographs based on the water balance principle, and the relationships between the design variable (the maximum discharge) and two flood variables (flood peak and volume) are determined.

The nonlinear reservoir model is schematically shown in Figure 1.  $\Omega$  is the reservoir area, which is assumed to increase continuously with the increase of water level  $H$  ( $H_0 = 0$  m at the beginning of flood discharge), and the reservoir volume  $V$  and discharge  $Q_{out}$  are also calculated from  $H_0 = 0$ .

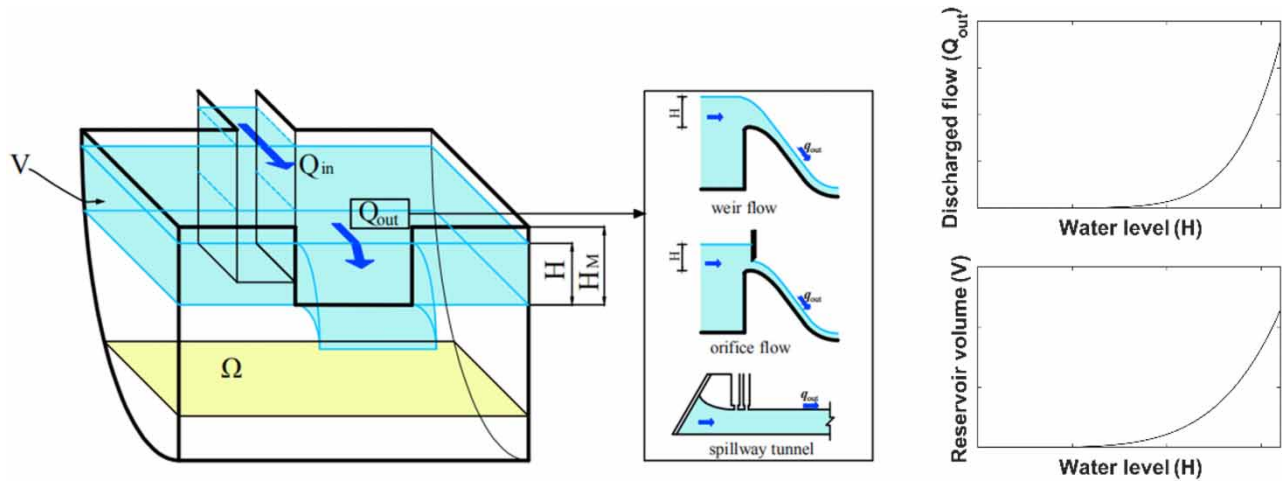


**Figure 1** | The nonlinear reservoir model.  $Q_{in}$  is the inflow hydrograph;  $\Omega$  is the reservoir area;  $V$  and  $H$  are the reservoir volume and water level above the spillway crest, respectively;  $H_M$  is the maximum water level during the routing process; and  $Q_{out}$  is the output hydrograph.

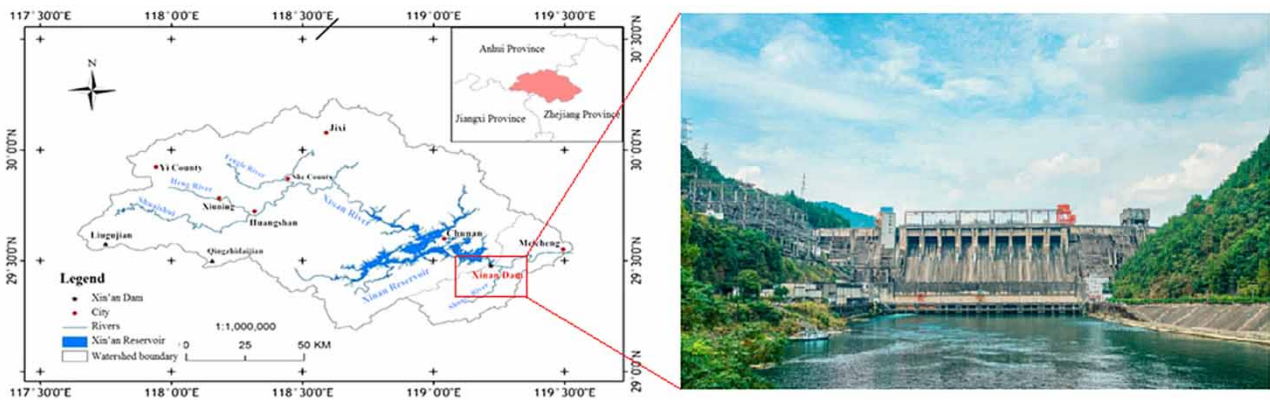


**Figure 2** | The river networks of Xin'an basin and the location of Xin'an reservoir.

As the reservoir volume-water level and discharge-water level relationships are assumed to be nonlinear, the relationship between reservoir volume  $V$  and water level  $H$  can be described as follows:

$$V = K_1 H^{n/m} \tag{7}$$

where  $V$  and  $H$  are the reservoir volume and water level above the spillway crest, respectively.

The relationship between the reservoir discharge  $Q_{out}$  and the water level  $H$  is:

$$Q_{out} = K_2 H^{1/m} \tag{8}$$

where  $Q_{out}$  is the output hydrograph.

It is known that  $1/m$  is associated with different discharge structures, which is often taken to be  $1/m = 0.5$  for orifice outflow and  $1/m = 1.5$  for weir flow in fitting the discharge capacity curves. In this study,  $1/m$  is set to range from 0.5 to 2 due to the use of multiple discharge structures.

Equations (7) and (8) are combined, and let  $K = K_1/K_2^m$ :

$$V = K Q_{out}^n \tag{9}$$



$Q_{in}$  is the inflow hydrograph, which is assumed to have a rectangular shape (Volpi & Flori 2014):

$$Q_{in} = \begin{cases} Q_{max} & t \leq t_i \\ 0 & t > t_i \end{cases} \quad (10)$$

where  $Q_{in}$  is the inflow hydrograph, and  $Q_{max}$  is the peak flow.

The water balance equation is:

$$Q_{in} - Q_{out} = \frac{dV}{dt} \quad (11)$$

Then, the following nonlinear differential equation can be obtained:

$$\frac{dQ_{out}}{dt} = \frac{1}{Kn} Q_{in} Q_{out}^{1-n} - \frac{1}{Kn} Q_{out}^{2-n} \quad (12)$$

Equation (12) can be solved using polynomial integration, approximate polynomial integration, and incomplete beta function. Here, the approximate polynomial integration method (Bender & Orszag 1999) is used to derive the relationships among flood peak, flood volume, design discharge, and maximum storage capacity of the reservoir due to its relatively simple expression.

$$\frac{dQ_{out}}{dt} + \frac{1}{Kn} Q_{out}^{2-n} = \frac{1}{Kn} Q_{in} Q_{out}^{1-n} \quad (13)$$

$$\frac{Q_{max}}{Kn} dt = Q_{out}^{n-1} \left( \frac{1}{1 - \frac{Q_{out}}{Q_{max}}} \right) dQ_{out} \quad (14)$$

Series expansion:

$$\frac{Q_{max}}{Kn} dt = Q_{out}^{n-1} \left( \left( \frac{Q_{out}}{Q_{max}} \right)^0 + \left( \frac{Q_{out}}{Q_{max}} \right)^1 + \left( \frac{Q_{out}}{Q_{max}} \right)^2 + \dots + \left( \frac{Q_{out}}{Q_{max}} \right)^r \right) dQ_{out} \quad (r \rightarrow \infty) \quad (15)$$

$$\frac{Q_{max}}{Kn} dt = \left( Q_{out}^{n-1} + \frac{Q_{out}^n}{Q_{max}} + \frac{Q_{out}^{n+1}}{Q_{max}^2} + \dots + \frac{Q_{out}^{n-1+r}}{Q_{max}^r} \right) dQ_{out} \quad (r \rightarrow \infty) \quad (16)$$

Integration of both sides yields:

$$\frac{Q_{max}t}{Kn} = \frac{Q_{out}^n}{n} + \frac{Q_{out}^{n+1}}{(n+1)Q_{max}} + \frac{Q_{out}^{n+2}}{(n+2)Q_{max}^2} \dots + \frac{Q_{out}^{n+r}}{(n+r)Q_{max}^r} \quad (r \rightarrow \infty) \quad (17)$$

$$\frac{Q_{max}t}{Kn} = \frac{Q_{out}^n}{n} + Q_{out}^n \sum_{i=1}^{\infty} \frac{1}{(n+i)Q_{max}^i} \quad (18)$$

$1/n + i$  can be approximated as  $1/i$ :

$$\frac{Q_{max}t}{Kn} = \frac{Q_{out}^n}{n} + Q_{out}^n \sum_{i=1}^{\infty} \frac{1}{i} \left( \frac{Q_{out}}{Q_{max}} \right)^i \quad (19)$$

$$Q_{max}t = KQ_{out}^n \left( 1 - n \ln \left( 1 - \frac{Q_{out}}{Q_{max}} \right) \right) \quad (20)$$

When  $t = t_i$ ,  $Q_{out}$  in Equation (20) gets the maximum value  $Q_{out,max}$ :

$$Q_{max}t_i = KQ_{out,max}^n \left( 1 - n \ln \left( 1 - \frac{Q_{out,max}}{Q_{max}} \right) \right) \tag{21}$$

The flood volume  $W = Q_{max}t_i$  can be obtained from Equation (10), and the maximum reservoir volume  $V_{max} = KQ_{out,max}^n$  during the routing process can be obtained from Equation (9):

$$W = V_{max} \left( 1 - n \ln \left( 1 - \frac{Q_{out,max}}{Q_{max}} \right) \right) \tag{22}$$

where  $W$  is the flood volume, and  $V_{max}$  is the maximum reservoir volume during the routing process.

The maximum reservoir discharge  $Q_{out,max}$  can be obtained for each inflow hydrograph using Equation (22). For a given return period  $T$  of the maximum discharge, the maximum design discharge  $Q_D$  can be described as:

$$Q_D = F_{Q_{out,max}}^{-1} \left( 1 - \frac{1}{T} \right) \tag{23}$$

where  $\mu = 1$ .

According to the mathematical model described in Section 2,  $Q_D$  is the design parameter, and  $Q_{in}$  and  $W$  are random variables which take into consideration the hydrological loads acting on the structure. The structure function is shown in Equation (22). Then, the probability distribution function of  $Q_D$  can be obtained, and the boundary of the integration region  $D_z$  is:

$$W = \gamma(Q_D) = V_{max} \left( 1 - n \ln \left( 1 - \frac{Q_{out,max}}{Q_{max}} \right) \right) \tag{24}$$

Let the maximum design discharge be the same as the maximum discharge in Equation (24), and thus  $Q_{out,max} = Q_D$ . The function has two asymptotes:  $W \rightarrow \infty$  as  $Q_{in} \rightarrow Q_{out,max}$  and  $Q_{in} \rightarrow \infty$  as  $W \rightarrow V_{max}$ . It follows from Equation (22) that the same  $Q_{out,max}$  can be derived from the limiting cases of the inflow hydrograph, which is characterized by an infinite peak flow but with a constant flood volume equal to  $V_{max}$ , or by an infinite flood volume but with a constant peak flow equal to  $Q_{out,max}$ .

Equation (24) can be rewritten as:

$$F_{Q_{out,max}}(q_{max}) = \int_{Q_{out,max}}^{\infty} \int_{V_{max}}^{\gamma(Q_{in})} f_{Q_{in},W}(q_i, w_i) dW dQ_{in} + F_W(V_{max}) + F_{Q_{in}}(Q_{out,max}) - \int_{-\infty}^{Q_{out,max}} \int_{-\infty}^{V_{max}} f_{Q_{in},W}(q_i, w_i) dW dQ_{in} \tag{25}$$

$F_{Q_{out,max}}(q_{max})$  is the probability distribution function of the maximum design discharge  $Q_{out,max}$ ;  $f_{Q_{in},W}(q_{in}, w_i)$  is the joint probability density function of random variables  $Q_{in}$  and  $W$ , where  $F_{Q_{in}}$  and  $F_W$  are their marginal distribution functions, respectively. When the design variable  $Q_{out,max}$  is independent of one of the two random variables (e.g.,  $W$ ), the boundary of  $D_z$  can be described as a straight line  $q_i = Q_{out,max}$ , and thus  $F_{Q_{out,max}} = F_{Q_{in}}$ .

It is important to note that the reservoir discharge-water level relationship remains approximately constant during the routing process, and both the maximum water level at the dam and the maximum reservoir volume can be achieved once the maximum discharge is achieved, which strictly corresponds to the structure return period.

#### 4. CASE STUDY

The Xin'an reservoir is located on the tributary of the Qiantang River in Tongguan Xia, Zhejiang Province, China Figure 2, and the upstream river is 323 km long with a drainage area of 10,442 km<sup>2</sup>. This reservoir is intended for flood control and power generation, and it has a multiyear regulation capacity with a normal pool level of 108 m and a storage capacity of 17.84 billion m<sup>3</sup>. The main discharge structure of the reservoir is the spillway with nine sluice gates, where the net width

of the spillway is 117 m, and the elevation of the spillway crest is 99 m. The flood data of the Luotongbu Station, the inflow observation station of the reservoir, for the period 1961–2008 were collected, from which the annual maximum flood peak flow  $Q_{\max}$  and the annual maximum 10-d flood volume  $W_{10}$  were extracted.

#### 4.1. Marginal and joint distributions

The marginal distribution functions of  $Q_{\max}$  and  $W_{10}$  are derived. The generalized extreme value (GEV) distribution is used in this study as the marginal distribution function due to its wide use and good performance in flood frequency analysis. The Gumbel copula is considered to best represent the relationship between peak and volume (Zhang & Singh 2006). Three copulas (G–H, Frank, and Clayton) from the Archimedean copula family are used in this study to simulate  $Q_{\max}$ – $W_{10}$  joint distribution, and the maximum likelihood method is used to estimate the parameter  $\theta$ . The optimal copula function is selected using Akaike information criterion (AIC), Bayesian information criterion (BIC) and root-mean-square error (RMSE), and the smaller the values of RMSE, AIC and BIC, the better the fitting of the copula function. Table 1 shows that the smallest AIC and BIC values are obtained by G–H copula, but its RMSE value is slightly larger than that of Frank copula. Thus, the G–H copula is used to describe the  $Q_{\max}$ – $W_{10}$  joint distribution in this study.

#### 4.2. Structure return period analysis

In this study, the maximum water level in the reservoir above the spillway crest  $H_{\max}$  is taken as the structure design variable. A nonlinear reservoir model is established, and then the structure return period is calculated and compared with that obtained based on a linear reservoir model.

##### 4.2.1. Structure return period based on the nonlinear reservoir model

###### (1) Reservoir volume–water level relationship

The elevation of the spillway crest of the Xin'an reservoir (99 m) is taken as the reference, at which the water level at the dam is  $H = 0$  m and the reservoir volume is  $V = 0$  m<sup>3</sup>. Then, the reservoir volume–water level relationship is fitted and described as follows:

$$V = 4.3341H^{1.1} \quad (26)$$

###### (2) Reservoir discharge–water level relationship

The water of the Xin'an reservoir is discharged mainly through an overflow spillway with a typical WES profile. This permits a free outflow without side contraction and marching of water head, and the water level at the dam–discharge relationship is fitted and described as follows:

$$Q_{\text{out}} = 264.31H^{3/2} \quad (27)$$

###### (3) Reservoir discharge–volume relationship

The discharge–reservoir volume relationship is obtained from Equations (26) and (27):

$$V = 0.07256Q_{\text{out}}^{11/15} \quad (28)$$

**Table 1** | Parameters of the  $Q_{\max}$ – $W_{10}$  joint distribution

Functions	$\theta$	AIC	BIC	RMSE
G–H copula	2.8506	–283.49	–278.16	0.0477
Clayton copula	2.6746	–279.73	–274.72	0.0499
Frank copula	10.5565	–254.15	–259.55	0.0386



## (4) Structural function

Substitution of Equation (28) into the water balance Equation (11) yields:

$$W_{10} = 4.3341H_{\max}^{1.1} \left( 1 - \frac{11}{15} \ln \left( 1 - \frac{264.31H_{\max}^{3/2}}{Q_{\text{in}}} \right) \right) \quad (29)$$

which is also the expression of the boundary of the integration region  $D_Z$  of  $H_{\max}$ .

The probability of  $D_Z$  at a given  $h_{\max}$  can be calculated from Equation (29), and then the structure return period is determined to be:

$$T_{n,s} = \frac{1}{1 - F_{H_{\max}}(h_{\max})} \quad (30)$$

**4.2.2. Structure return period based on the linear reservoir model**

The structure return period based on the linear reservoir model in which both reservoir volume-water level and discharge-water level relationships are assumed to be linear is also calculated following the same procedure and compared with that based on the nonlinear model (see Volpi & Flori (2014) and Balistrocchi *et al.* (2017) for details).

The linear reservoir water level–volume relationship can be simulated using the measured reservoir volume and water level data:

$$V = 5.5791H \quad (31)$$

The linear reservoir water level–discharge relationship is:

$$Q_{\text{out}} = 974.11H \quad (32)$$

The linear reservoir volume–discharge relationship is:

$$V = 0.00573Q_{\text{out}} \quad (33)$$

The structure function is:

$$W_{10} = -0.00573Q_{\text{in}} \ln \left( 1 - \frac{974.11H_{\max}}{Q_{\text{in}}} \right) \quad (34)$$

Then,

$$T_{l,s} = \frac{1}{1 - F_{H_{\max}}(h_{\max})} \quad (35)$$

**4.3. Comparison of structure return periods between linear and nonlinear models**

In this section, the structure return periods based on linear and nonlinear reservoir models are calculated and compared, and possible explanations of the difference are discussed.

Figure 3(a) shows the comparison of the maximum water level–return period relationships between linear and nonlinear models. It shows that when  $T < 360\text{a}$ , the  $H_{\max}$  of the nonlinear model is larger than that of the linear model at the same return period; while the opposite trend is observed when  $T > 360\text{a}$ . As the  $H_{\max}$  value increases, the  $T$  value of the nonlinear model increases more rapidly, which can be attributed to the more rapid change of  $Q_{\text{out,max}}$  and  $V_{\text{max}}$  with  $H_{\max}$ , as shown in Figure 3(b).

Six representative return periods ( $T = 10, 50, 100, 200, 500,$  and  $1,000\text{a}$ ) are selected for further analysis, and Table 2 shows the  $H_{\max}$ ,  $Q_{\text{out,max}}$ , and  $V_{\text{max}}$  at different return periods for linear and nonlinear models. It is found that the  $H_{\max}$  values of the linear model are smaller than that of the nonlinear model at  $T = 10, 50,$  and  $100\text{a}$ , while the opposite is true for the values of  $Q_{\text{out,max}}$  and  $V_{\text{max}}$ . The values of  $H_{\max}$ ,  $Q_{\text{out,max}}$ , and  $V_{\text{max}}$  increase with the increase of the return period, which, however, is

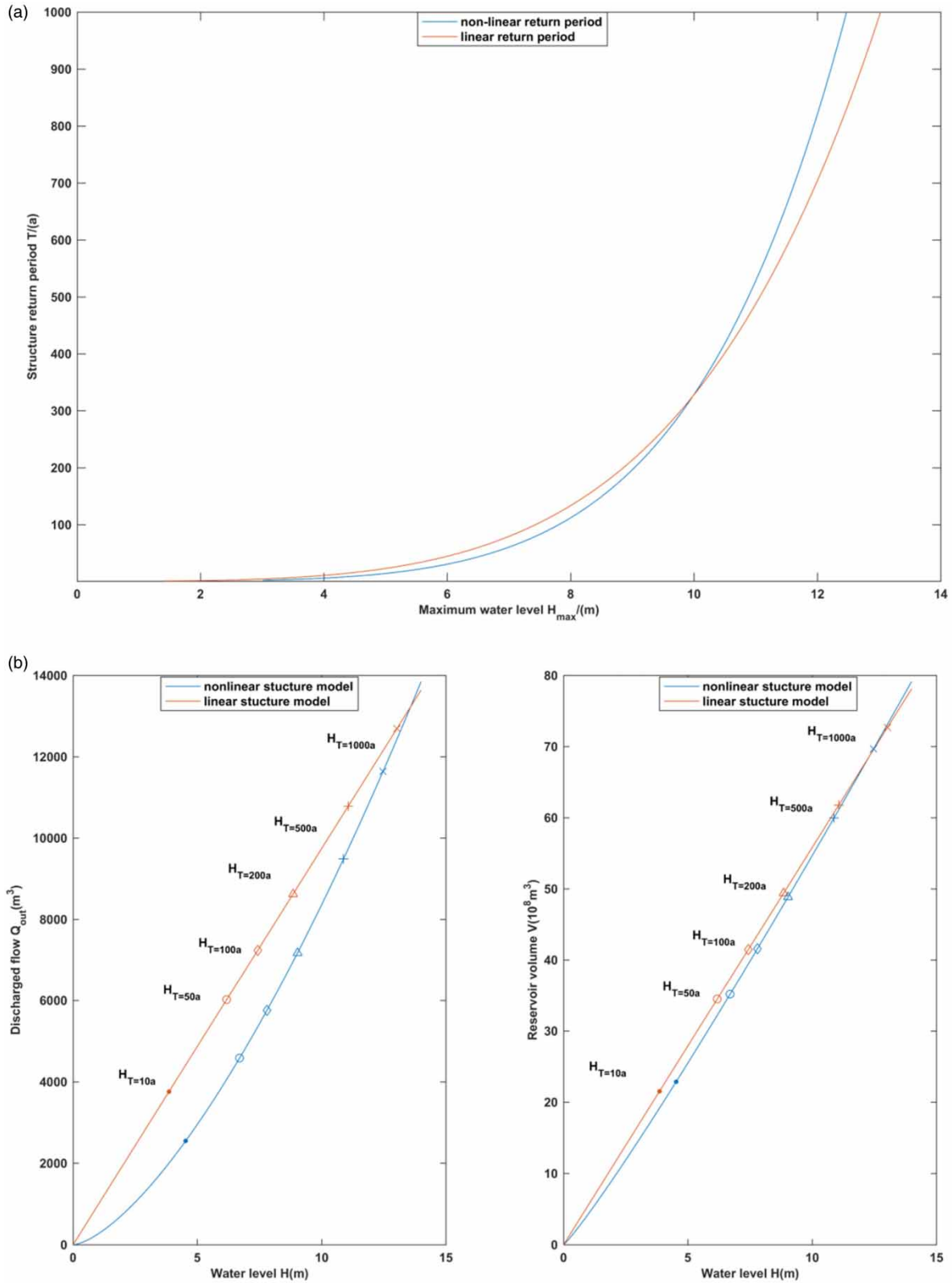


**Figure 3** | Comparison of the relationships of the maximum water level with (a) the return period and (b) the maximum discharge and volume between linear and nonlinear models.

**Table 2** | The maximum water level, maximum discharge, and maximum volume of the reservoir at different return periods for linear and nonlinear models

Return period (Ts/a)	Maximum water level ( $H_{\max}$ /m)		Maximum discharge ( $Q_{\text{out, max}}$ /(m <sup>3</sup> /s))		Maximum reservoir volume ( $V_{\max}$ /10 <sup>8</sup> m <sup>3</sup> )	
	Nonlinear model	Linear model	Nonlinear model	Linear model	Nonlinear model	Linear model
10	4.53	3.86	2,551.91	3,763.13	22.86	21.55
50	6.70	6.18	4,585.34	6,022.19	35.13	34.49
100	7.80	7.43	5,761.66	7,233.86	41.54	41.43
200	9.03	8.85	7,175.06	8,623.39	48.79	49.39
500	10.88	11.07	9,486.47	10,778.60	59.87	61.73
1,000	12.47	13.03	11,643.84	12,688.00	69.58	72.67

**Table 3** | The maximum water levels at the dam at different return periods under non-stationary and stationary conditions based on the nonlinear storage/discharge model

Return period (Ts/a)	Non-stationary conditions					Stationary conditions
	1961	1971	1981	1991	2001	
10	4.02	4.22	4.43	4.66	4.89	4.53
50	4.94	5.19	5.45	5.72	6.01	6.70
100	5.26	5.52	5.81	6.10	6.41	7.80
200	5.55	5.83	6.12	6.43	6.75	9.03
500	5.88	6.18	6.48	6.81	7.16	10.88
1,000	6.10	6.41	6.73	7.07	7.43	12.47

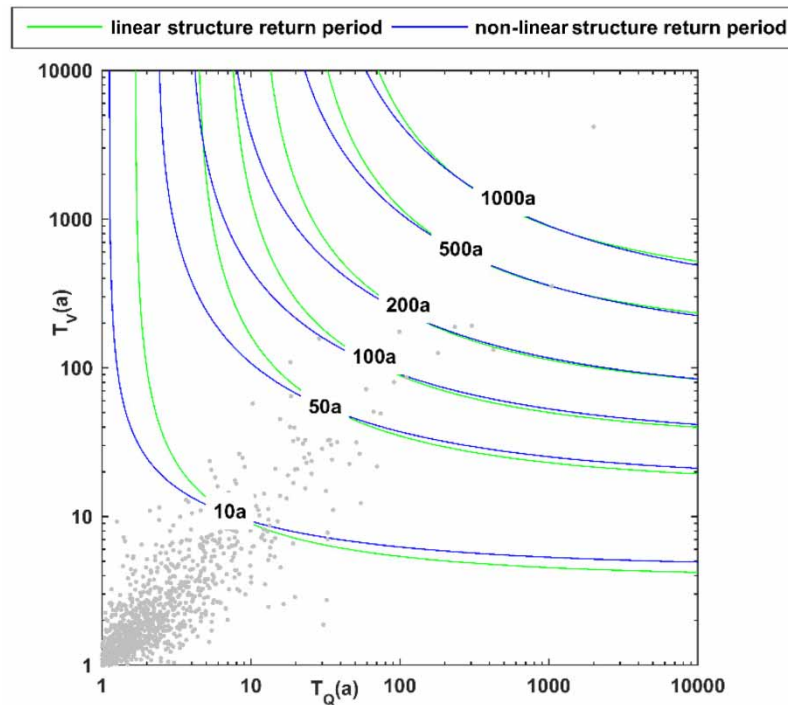
more pronounced for the linear model. This is because the discharge changes more rapidly with the water level for the nonlinear model, as shown in the  $Q_{\text{out, max}}-H$  curve. At a return period of 500 years, the values of  $H_{\max}$ ,  $Q_{\text{out, max}}$ , and  $V_{\max}$  of the linear model are larger than those of the nonlinear model, indicating that flood risk is over-estimated by the linear model.

Figure 4 shows the comparison of the structure return period isolines at  $T = 10, 50, 100, 200, 500,$  and  $1,000\text{a}$  between linear and nonlinear reservoir models, and gray dots are the 1,000 random combinations of flood peak and volume generated using the G–H copula. It is important to note that any flood event on the same isoline would produce the same maximum reservoir volume, maximum water level at the dam, and maximum discharge, and thus have the same impact on the reservoir. However, given their different assumptions about the reservoir volume–water level and discharge–water level relationships, the boundary of the supercritical region differs substantially between linear and nonlinear reservoir models, resulting in substantial differences in the isolines at the same return period. It is seen that at a return period of  $T = 10, 50, 100,$  and  $200\text{a}$ , the discharge for the linear reservoir model is higher compared with that for the nonlinear reservoir model, and the nonlinear reservoir model is more sensitive to floods with high flood peak but low flood volume; whereas at a return period of  $T = 500\text{a}$  and  $T = 1,000\text{a}$  at which the maximum water level at the dam is high, the discharge and volume are approximately the same between linear and nonlinear reservoir models, and as a result the isolines are approximately coincident with each other.

It is thus concluded that reservoir discharge and volume would be increased to different extents with increasing water level for linear and nonlinear reservoir models due to their differences in the reservoir volume–water level and discharge–water level curves, which consequently have an effect on the structure return period. In addition, the reservoir volume–water level and discharge–water level curves can also have an effect on the boundary of the supercritical region, thus resulting in differences in the isolines at the same return period between linear and nonlinear reservoir models.

#### 4.4. Comparison of different return periods

For the Kendall return period, the supercritical region is defined as the region enveloped by the isoline of the joint return period. Here, the structure return period which is applicable to the flood control structures and the Kendall return period



**Figure 4** | The isolines of the structure return periods for linear and nonlinear models.

which is applicable to natural occurrence of floods are compared. The isolines of the structure return period and the Kendall return period at a return period of  $T = 10, 50, 100, 200, 500,$  and  $1,000a$  are shown in Figure 5, and gray dots in Figure 5 are the 1,000 random combination of flood peak and volume generated using the G–H copula.

It shows that the Kendall return period isoline is symmetric about the straight line with an angle of  $45^\circ$ , as it is based on the joint return period; while the symmetry axis of the structure return period isoline is more inclined to the y-axis, which is affected by the reservoir structure such that a flood event with a larger peak flow can pose a greater risk to the reservoir structure.

There are an infinite number of peak–volume pairs at the same Kendall return period, which can produce different reservoir responses and thus pose different levels of risk to the flood control structures. The Kendall return period of  $T = 10a$  is analyzed. It is noted that the isoline with a Kendall return period of  $T = 10a$  intersects that with a structure return period of  $10, 50,$  and  $100a$ , which are denoted as points A, B, C, and D. The occurrence probability of floods at points A, B, C, and D is  $10a$ ; the return period of the maximum water level at the dam for peak–volume pairs at points A and D is also  $10a$ ; while that at points B and C is  $50$  and  $100a$ , respectively. Thus, the maximum water level in response to peak–volume pairs on the left side of point A and the right side of point D on the Kendall return period isoline of  $T = 10a$  is higher than  $10a$ , while that between points A and D is lower than  $10a$ . It is concluded that the reservoir would respond differently to different peak–volume pairs at the same Kendall return period, and thus flood risk is likely to be substantially underestimated in some circumstances. At a Kendall return period of  $T = 10a$ , the maximum reservoir response is  $196.34a$  and the minimum reservoir response is  $8.96a$ .

The Kendall return period is often used in bivariate design, and the maximum likelihood method, the most likely composition method, and the same frequency method are used for flood peak and volume estimation. The bivariate design based on the Kendall return period accounts for the natural occurrence of floods without considering the effects of hydraulic structures during the routing process, which can lead to over- or underestimation of flood risk from the perspective of hydraulic structure safety.

## 5. DISCUSSION

Although the nonlinear reservoir model has been successfully applied to the Xin'an Reservoir, other reservoirs may show quite different reservoir volume–water level and discharge–water level relationships ( $V = K_1 H^{n/m}$  and  $Q_{out} = K_2 H^{1/m}$ ). Thus, the effects of the four parameters ( $K_1, n/m, K_2,$  and  $1/m$ ) on the results are analyzed to verify the applicability of the proposed model to other hydraulic structures.

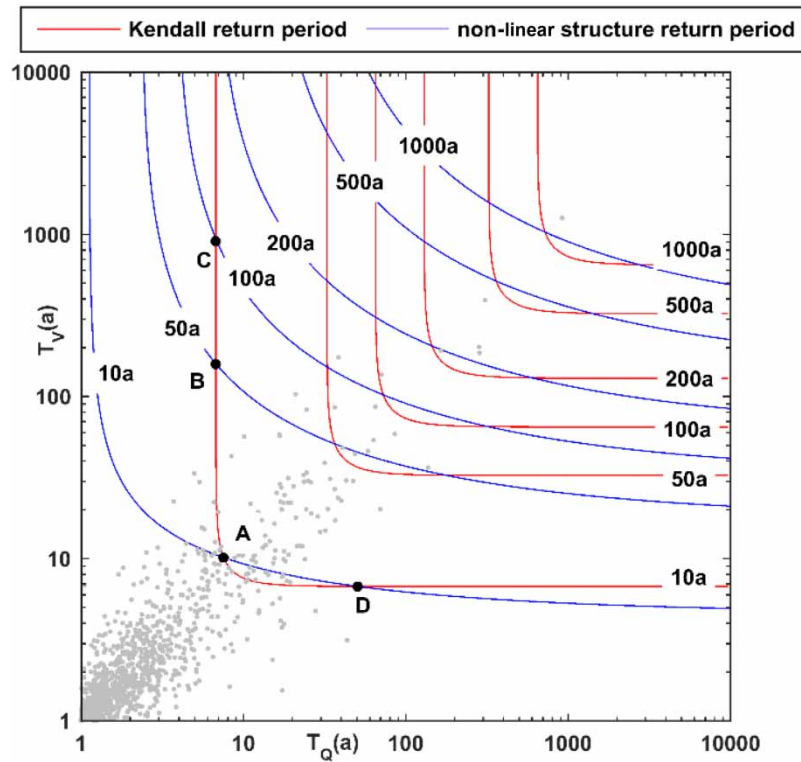


**Figure 5** | Comparison of the nonlinear structure return period and the Kendall return period.

### 5.1. Effects of parameters of the discharge capacity curves

The discharge capacity of a reservoir depends largely on the spillway length and discharge regime, which correspond to  $K_2$  and  $1/m$  in Equation (8), respectively. Specifically,  $1/m$  indicates the discharge capacity of the reservoir under different discharge regimes, which can be affected not only by the structure, such as sluice gate and overflow weir, but also by flow patterns such as orifice and weir outflow through the sluice gate. In general, the larger the discharge capacity is, the larger the  $1/m$  value will be.  $K_2$  indicates the spillway length, and the larger the spillway length is, the larger the  $K_2$  value will be. Here, a constant reservoir volume-water level relationship is considered ( $V = H^{1.1}$ ), and the effects of  $K_2$  (100, 200, and 300) and  $1/m$  (0.5, 1, 1.5, and 2) on the discharge capacity ( $Q_{\text{out}} = K_2 H^{1/m}$ ) are investigated.

Figure 6 shows the relationships between the structure return period ( $T$ ) and the maximum water level ( $H_{\text{max}}$ ) for different discharge curves. It shows that at the same structure return period  $T$ , an increase in  $K_2$  or  $1/m$  can lead to an increase in the discharge capacity and consequently a decrease in  $H_{\text{max}}$ . However, it is important to note that there is a nonlinear relationship between  $T$  and  $H_{\text{max}}$ , and  $T$  increases at an increasing rate with the increase of  $H_{\text{max}}$ .

As  $1/m$  indicates the discharge capacity of the reservoir under different discharge regimes, it can have a significant effect on the return period. For instance, as  $1/m$  is increased by 100, 50, and 33.3% from  $1/m_1 = 0.5$  ( $Q = 100H^{0.5}$ ) to  $1/m_2 = 1$  ( $Q = 100H$ ),  $1/m_3 = 1.5$  ( $Q = 100H^{1.5}$ ), and  $1/m_4 = 2$  ( $Q = 100H^2$ ) at  $K_2 = 100$ , the  $H_{\text{max}}$  is decreased by 10.9, 23.4, and 34.3% from  $h_1 = 19.49$  m to  $h_2 = 17.38$  m,  $h_3 = 13.30$  m, and  $h_4 = 8.74$  m at  $T = 10a$ , respectively. Under the same  $K_2$  conditions, the structure return period for the same  $H_{\text{max}}$  would increase at an increasing rate with the increase of  $1/m$ . This is because the discharge capacity of the reservoir is increased as the  $H_{\text{max}}$  increases, and thus the larger the  $1/m$  value is, the higher the increase rate of the discharge capacity of the reservoir will be.

It is also noted that  $K_2$ , which is used to indicate the increase or decrease in the spillway length, can also have an effect on the  $H_{\text{max}} \sim T$  relationship. For instance, as  $K_2$  is increased by 100 and 50% from  $k_{2,1} = 100$  ( $Q = 100H^{0.5}$ ) to  $k_{2,2} = 200$  ( $Q = 200H^{0.5}$ ), and  $k_{2,3} = 300$  ( $Q = 300H^{0.5}$ ) at  $T = 10a$  and  $1/m = 0.5$ , the  $H_{\text{max}}$  is decreased by 9.1 and 8.0% from  $h_1 = 19.49$  m to  $h_4 = 17.72$  m and  $h_5 = 16.30$  m, respectively. Under the same  $1/m$  conditions, the structure return period for the same  $H_{\text{max}}$  would also increase at an increasing rate with the increase of  $K_2$ . Again, this is because the discharge capacity of the reservoir is increased as the  $H_{\text{max}}$  increases, and thus the larger the  $K_2$  value is, the higher the increase rate of the discharge capacity of the reservoir will be.

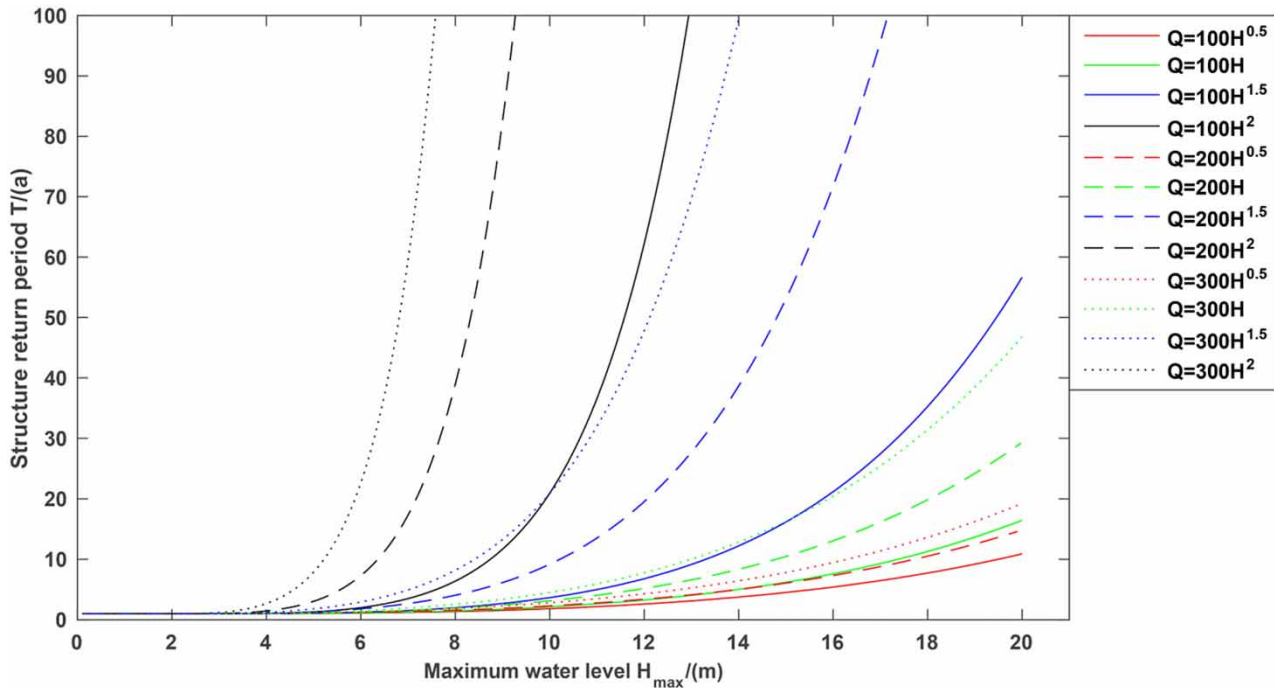


**Figure 6** | The relationship between the structure return period and the maximum water level for different parameters of the discharge capacity curves.

## 5.2. Effects of parameters of reservoir volume and water level curves

The relationship between reservoir water level and its volume is closely associated with the geographical location and characteristics of the reservoir, which can also have an effect on the structure return period. Under the conditions of  $Q_{\text{out}} = 250H^{1.5}$ , the effects of parameters  $K_1$  ( $K_1 = 1, 1.5, 2, \text{ or } 3$ ) and  $n/m$  ( $n/m = 1, 1.2, 1.5, \text{ or } 2$ ) in  $V = K_1H^{n/m}$  are discussed.

Figure 7 shows the  $H_{\text{max}} \sim T$  relationships for different reservoir volumes. At the same structure return period, an increase in  $K_1$  or  $n/m$  can lead to an increase in the storage capacity and consequently a decrease in  $H_{\text{max}}$ . It is also note that the relationship between  $T$  and  $H_{\text{max}}$  is nonlinear, and  $T$  increases at an increasing rate with the increase of  $H_{\text{max}}$ .

Note that as the storage capacity is mainly affected by the geographical location of the reservoir, it would be much more difficult to change than reservoir discharge capacity. Nevertheless, changes in reservoir storage capacity can have a substantial impact on the safety of hydraulic structures. For instance, under the conditions of  $n/m = 1.1$  ( $V = H^{1.1}$ ,  $V = 1.5H^{1.1}$ ,  $V = 2H^{1.1}$  and  $V = 3H^{1.1}$ ), an increase of  $K_1$  by 50, 100, and 200% results in a decrease in  $H_{\text{max}}$  by 12.1, 22.4, and 37.4% at  $T = 10a$ , respectively. Under the same  $n/m$  conditions, the structure return period for the same  $H_{\text{max}}$  would increase at an increasing rate with the increase of  $K_1$ . Again, this is because the storage capacity of the reservoir is increased as the  $H_{\text{max}}$  increases, and thus the larger the  $K_1$  value is, the higher the increase rate of the storage capacity of the reservoir will be.

For curves with  $K_1 = 1$  ( $V = H$ ,  $V = H^{1.1}$ ,  $V = H^{1.2}$ ,  $V = H^{1.5}$ , and  $V = H^2$ ), an increase of  $n/m$  by 10, 20, 50, and 100% results in a decrease in  $H_{\text{max}}$  by 5.6, 12.6, 33.0, and 54.2% at  $T = 10a$ , respectively. Under the same  $K_1$  conditions, the structure return period for the same  $H_{\text{max}}$  would increase at an increasing rate with the increase of  $n/m$ . Again, this is because the storage capacity of the reservoir is increased as the  $H_{\text{max}}$  increases, and thus the larger the  $n/m$  value is, the higher the increase rate of the storage capacity of the reservoir will be.

## 5.3 Analysis of the Xin'an reservoir under stationary and non-stationary conditions

Figure 8 shows the time series of the annual maximum flood peak flow  $Q_{\text{max}}$  and the annual maximum 10-d flood volume  $W_{10}$  recorded at the Luotongbu Station for the 48-year period 1961–2008. It is seen that both  $Q_{\text{max}}$  and  $W_{10}$  time series show an increasing trend for the period 1961–2008.

The annual flood peak and the annual maximum 10-d flood volume records at the Luotongbu Station for the period 1961–2008 were fitted based on the GAMLSS model and the parameters were estimated. Figure 9 shows the evolution of  $Q_{\text{max}}$  and  $W_{10}$  at a return period of 1,000, 500, 200, 100, 50, and 10 years for the period 1961–2008.



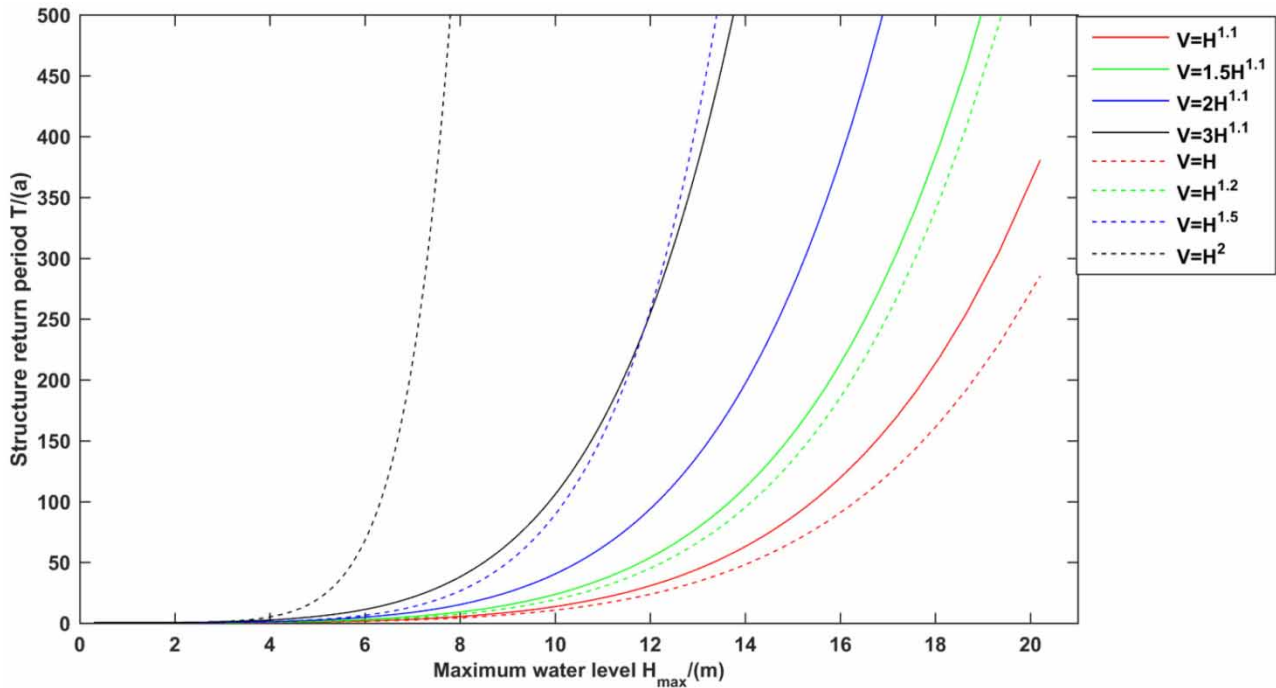


**Figure 7** | The relationship between the structure return period and the maximum water level for different parameters of reservoir volume and water level curves.

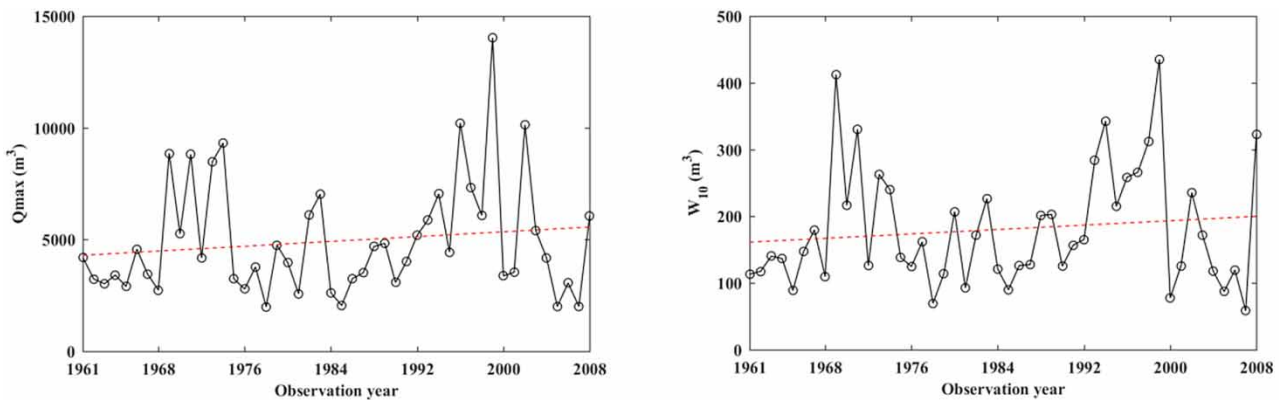


**Figure 8** | Time series of annual maximum flood peak flow  $Q_{max}$  and annual maximum 10-d flood volume  $W_{10}$  for the period 1961–2008.

The distribution functions of the peak flow and volume in 1961, 1971, 1981, 1991, and 2001 under non-stationary conditions are selected, and the non-linear model is applied to the Xin’an reservoir to verify its applicability under non-stationary conditions.

Figure 10 shows the relationships between the maximum water level at the dam and the return period under non-stationary and stationary conditions, and Figure 11 shows the marginal distributions of annual maximum flood peak flow  $Q_{max}$  and the annual maximum 10-d flood volume  $W_{10}$  under non-stationary and stationary conditions. It is seen from Figure 10 that under non-stationary conditions, the maximum water level at the dam  $H_{max}$  for the same return period also shows an increasing trend for the period 1961–2008; while the return period  $T$  for the same year increases at a higher rate with the increase of the maximum water level at the dam. However, it should also be noted that the increasing rate is higher under non-stationary conditions than that under stationary conditions as a result of the marginal distributions of annual maximum flood peak flow and annual maximum 10-d flood volume. As shown in Figure 11, higher flood peaks are more likely to occur under non-stationary conditions, which can cause more severe damage to the reservoir structure and consequently the return period.

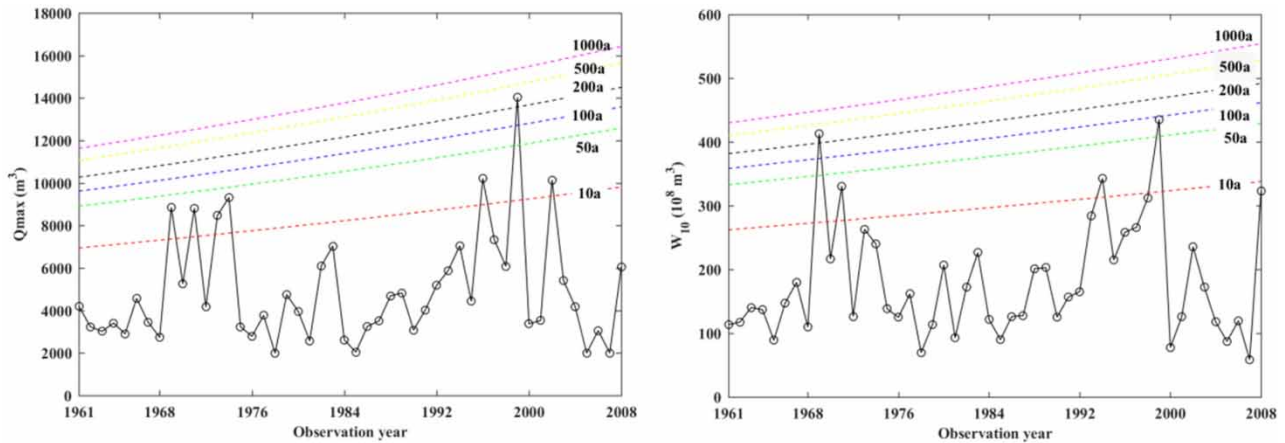


**Figure 9** | The evolution of annual maximum flood peak flow  $Q_{max}$  and annual maximum 10-d flood volume  $W_{10}$  at a return period of 1,000, 500, 200, 100, 50, and 10 years for the period 1961–2008.

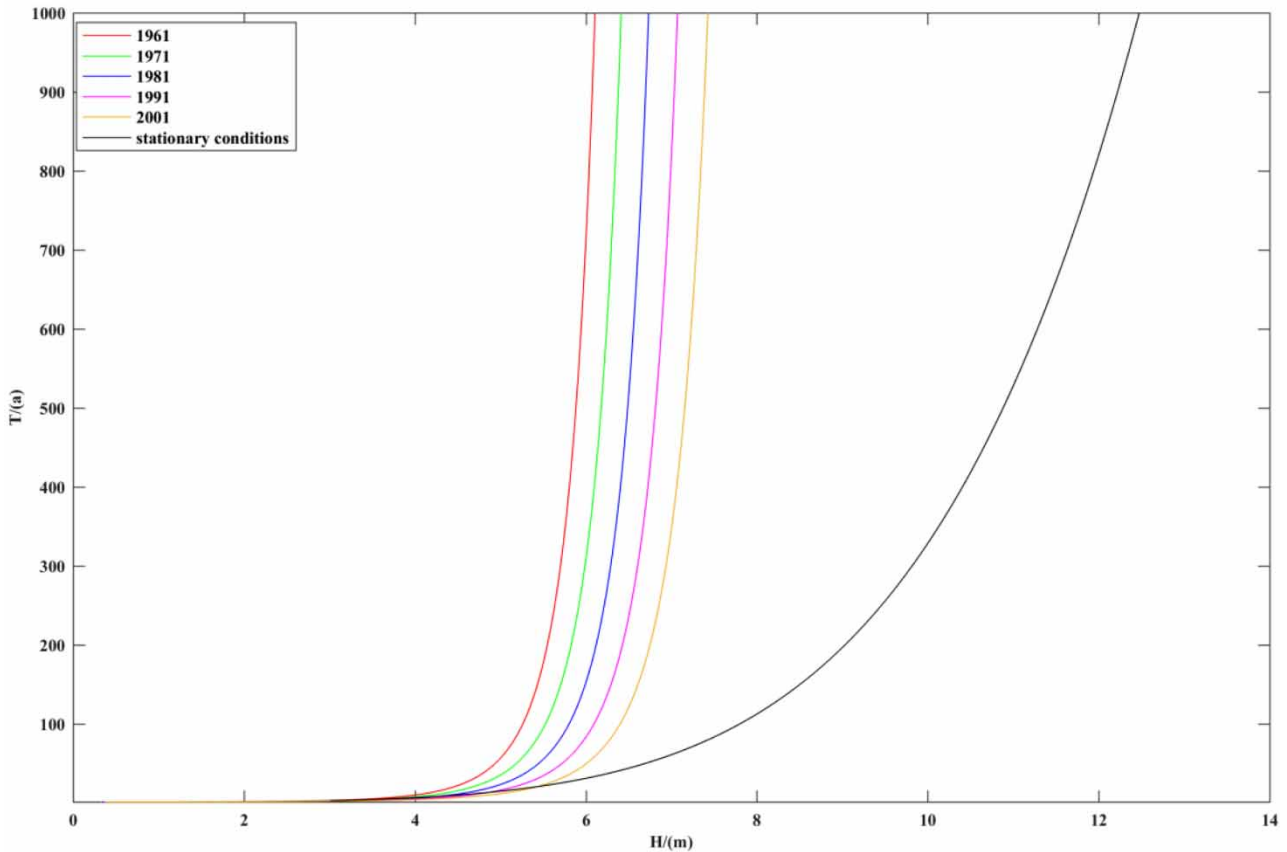


**Figure 10** | The relationships between the maximum water level at the dam and the return period under non-stationary and stationary conditions.

Six representative return periods ( $T = 10, 50, 100, 200, 500,$  and  $1,000a$ ) are considered for comparison [Table 3](#). Different  $Q_{max}$ - $W_{10}$  joint distributions are used to obtain the nonlinear return periods under non-stationary conditions, and the increasing trend of  $Q_{max}$  and  $W_{10}$  for the period 1961–2008 implies that there is a higher probability of the joint occurrence of large  $Q_{max}$  and  $W_{10}$ . Under conditions of constant reservoir volume-water level and discharge-water level relationships, a higher

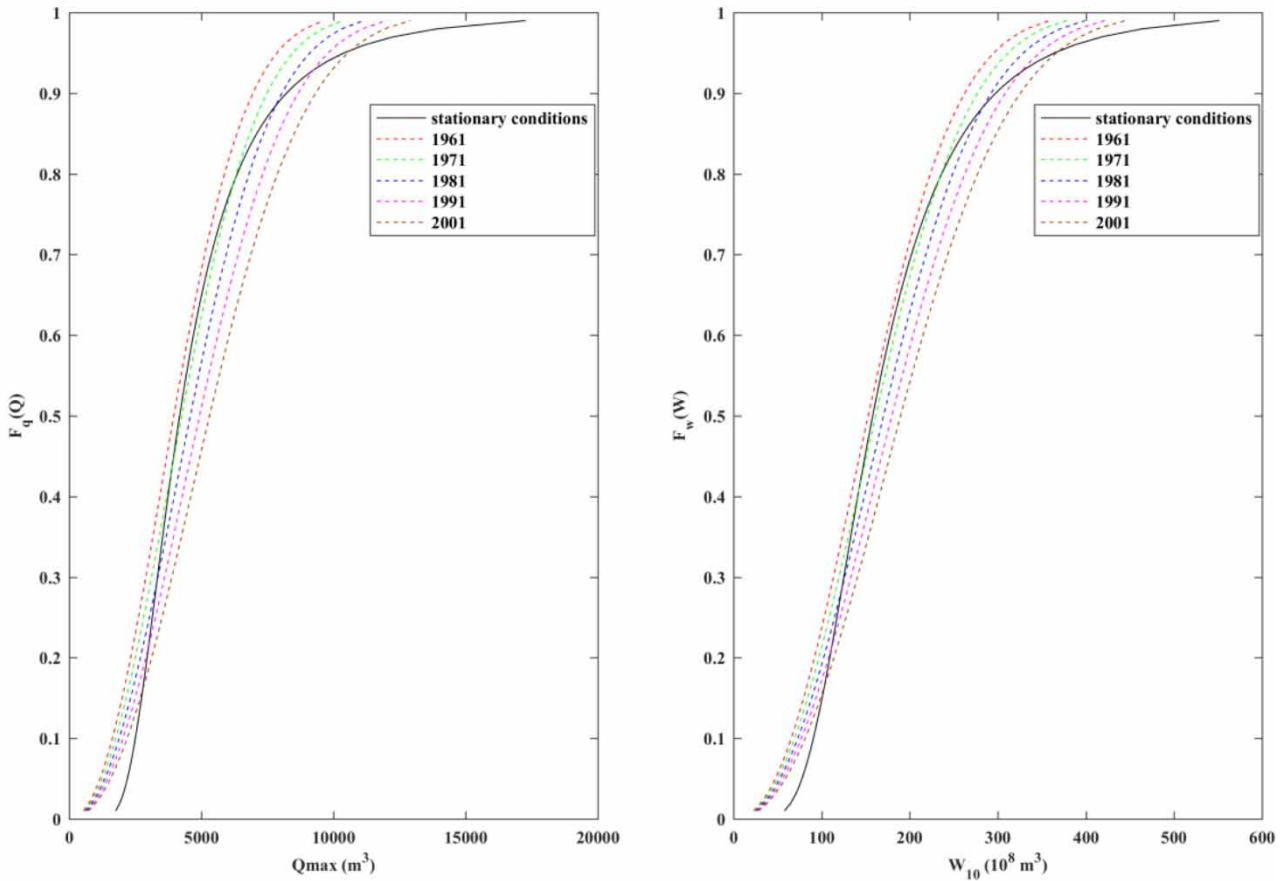


**Figure 11** | The marginal distributions of annual maximum flood peak flow  $Q_{\max}$  and the annual maximum 10-d flood volume  $W_{10}$  under non-stationary and stationary conditions.

maximum water level at the dam  $H_{\max}$  is more likely to occur, which in turn may cause more severe damage to the reservoir. At a return period of  $T = 10a$ , the probability of the  $Q_{\max}-W_{10}$  joint distribution under non-stationary conditions is similar to that under stationary conditions. Thus, under conditions of constant reservoir volume-water level and discharge-water level relationships, there would be no substantial difference in the return period between non-stationary and stationary conditions. However, the probability of the joint occurrence of large  $Q_{\max}$  and  $W_{10}$  would increase as the return period increases under non-stationary conditions because of the effects of the marginal distributions of annual maximum flood peak flow and annual maximum 10-d flood volume. In this case, the return periods obtained under stationary conditions are more conservative.

## 6. CONCLUSIONS

In this study, a general nonlinear reservoir model was proposed for the design and risk assessment of hydraulic structures in a bivariate context. A case study was then performed with the Xin'an reservoir, and the nonlinear structure return period was calculated and compared with the linear structure return period and the Kendall return period. The main conclusions are summarized as follows.

1. The supercritical region  $D_Z$  plays a determinant role in the design and risk assessment of hydraulic structures, and its boundary is affected by the structure and hydrological load acting on the structure. Thus, it is imperative to consider the structure and the way it interacts with the hydrological load in determining the structure function. In this study, a nonlinear reservoir model is established, and the relationship between structure and hydrological load is determined using the approximate polynomial integration method and then the supercritical region  $D_Z$  is obtained. Unlike the linear reservoir model, nonlinear reservoir volume-water level and discharge-water level relationships are assumed in this study, thus making it possible to capture the routing processes of the reservoir more accurately and flexibly.

2. The maximum water level at the dam is taken as the structure design variable, and the structure return period based on the nonlinear reservoir model is calculated and compared with that based on the linear reservoir model. Given their different assumptions about the reservoir volume-water level and discharge-water level relationships, the boundary of the supercritical region differs substantially between linear and nonlinear reservoir models, resulting in substantial differences in the structure return period. The change rates of discharge and reservoir volume with reservoir water level may also differ between linear and nonlinear reservoir models, and thus they show different levels of sensitivity to floods with different peak-volume combinations and thus lead to differences in the structure return period.
3. The structure-based multivariate return period is distinctively different from the hydrological event-based multivariate return period. The structure return period is more applicable than the Kendall return period to flood control structures as it takes into consideration the interactions of the structure and hydrological load acting on the structure. However, it is important to note that the Kendall return period can lead to over- or underestimation for hydraulic structures in multivariate flood frequency analysis.
4. For the nonlinear reservoir model, the effects of  $K_1$ ,  $n/m$ ,  $K_2$ , and  $1/m$  involved in the reservoir volume-water level and discharge-water level relationships ( $V = K_1 H^{n/m}$  and  $Q_{\text{out}} = K_2 H^{1/m}$ ) are investigated to verify the applicability of the proposed model. It is found that an increase in  $K_1$  or  $n/m$  leads to an increase in reservoir storage capacity; while an increase in  $K_2$  or  $1/m$  leads to an increase in reservoir discharge capacity. Different reservoirs would respond differently to the same flood event due to their different storage and discharge capacity, which can have an effect on the structure return period.

However, as it is difficult to derive the general solution of the nonlinear differential equation, the inflow hydrograph is simplified to be a constant process in this study, which may make the results less accurate. Efforts should also be made to better describe the fluctuation of the inflow hydrograph and to investigate the effects of the operation rules on the routing processes of the reservoir.

## ACKNOWLEDGEMENTS

This research is funded by the National Natural Science Foundation of China (52079040), the Fundamental Research Funds for the Central Universities (B210201023), and Jiangsu Water Science and Technology Project (2019027 and 2020065).

## DATA AVAILABILITY STATEMENT

All relevant data are included in the paper or its Supplementary Information.

## REFERENCES

- Balisticchi, M., Orlandini, S., Ranzi, R. & Bacchil, B. 2017 Copula-based modeling of flood control reservoirs. *Water Resour. Res.* **53**, 9883–9900. <https://doi.org/10.1002/2017WR021345>.
- Bender, C. M. & Orszag, S. A. 1999 *Advanced Mathematical Methods for Scientists and Engineers*. Springer, New York, NY.
- Chebana, F. & Ouarda, T. 2011 Multivariate quantiles in hydrological frequency analysis. *Environmetrics* **22**, 63–78. <https://doi.org/10.1002/env.1027>.
- De Michele, C., Salvadori, G., Canossi, M., Petaccia, A. & Rosso, R. 2005 Bivariate statistical approach to check adequacy of dam spillway. *J. Hydrol. Eng.-ASCE* **10**, 50–57. [https://doi.org/10.1061/\(ASCE\)1084-0699\(2005\)10:1\(50\)](https://doi.org/10.1061/(ASCE)1084-0699(2005)10:1(50)).
- Favre, A.-C., El Adlouni, S., Perreault, L., Thiemonge, N. & Bobee, B. 2004 Multivariate hydrological frequency analysis using copulas. *Water Resour. Res.* **40**, 1–12. <https://doi.org/10.1029/2003WR002456>.
- Klein, B., Pahlow, M., Hundecha, Y. & Schumann, A. 2010 Probability analysis of hydrological loads for the design of flood control systems using copulas. *J. Hydrol. Eng.-ASCE* **15**, 360–369. [https://doi.org/10.1061/\(ASCE\)HE.1943-5584.0000204](https://doi.org/10.1061/(ASCE)HE.1943-5584.0000204).
- Mediero, L., Jiménez-Álvarez, A. & Garrote, L. 2010 Design flood hydrographs from the relationship between flood peak and volume. *Hydrol. Earth Syst. Sci.* **14**, 2495–2505. <https://doi.org/10.5194/hess-14-2495-2010>.
- Nelsen, R. B. 2006 *An Introduction to Copulas*, 2nd edn. Springer, New York, NY.
- Requena, A., Mediero, L. & Garrote, L. 2015 A bivariate return period based on copulas for hydrologic dam design: accounting for reservoir routing in risk estimation. *Hydrol. Earth Syst. Sci.* **17**, 3023–3038. <https://doi.org/10.5194/hess-17-3023-2013>.
- Salvadori, G. & De Michele, C. 2004 Frequency analysis via copulas: theoretical aspects and applications to hydrological events. *Water Resour. Res.* **40**, 1–17. <https://doi.org/10.1029/2004WR003133>.
- Salvadori, G., De Michele, C. & Durante, F. 2011 On the return period and design in a multivariate framework. *Hydrol. Earth Syst. Sci.* **15**, 3293–3305. <https://doi.org/10.5194/hess-15-3293-2011>.

- Salvadori, G., Durante, F. & De Michele, C. 2013 Multivariate return period calculation via survival functions. *Water Resour. Res.* **49**, 2308–2311. <https://doi.org/10.1002/wrcr.20204>.
- Shiau, J., Wang, H. & Tsai, C. 2006 Bivariate frequency analysis of floods using copulas. *J. Am. Water Resour. Assoc.* **42**, 1549–1564. <https://doi.org/10.1111/j.1752-1688.2006.tb06020.x>.
- Volpi, E. & Fiori, A. 2014 Hydraulic structures subject to bivariate hydrological loads: return period, design, and risk assessment. *Water Resour. Res.* **50**, 885–897. <https://doi.org/10.1002/2013WR014214>.
- Yan, L., Xiong, L., Guo, S., Xu, C.-Y., Xia, J. & Du, T. 2017 Comparison of four nonstationary hydrologic design methods for changing environment. *J. Hydrol.* **551**, 132–150.
- Yan, L., Xiong, L., Luan, Q., Jiang, C., Yu, K. & Xu, C.-Y. 2020 On the applicability of the expected waiting time method in nonstationary flood design. *Water Resour. Manag.* **34**, 2585–2601.
- Zhang, L. & Singh, V. P. 2006 Bivariate flood frequency analysis using the copula method. *J. Hydrol. Eng.-ASCE* **11**, 150–164. [https://doi.org/10.1061/\(ASCE\)1084-0699\(2006\)11:2\(150\)](https://doi.org/10.1061/(ASCE)1084-0699(2006)11:2(150)).

First received 27 July 2021; accepted in revised form 31 July 2021. Available online 1 September 2021